Journal of Applied Polymer Science

Effect of Phenol End Functional Switching Segments on the Shape Memory Properties of Epoxy-Cyanate Ester System

R. Biju,[1] C. P. Reghunadhan Nair[2]

[1]Sree Narayana College, Sivagiri, Varkala, Thiruvananthapuram 695 145, Kerala, India

[2]Polymers and Special Chemicals Group, Vikram Sarabhai Space Centre, Thiruvananthapuram 695 022, Kerala, India

Correspondence to: R. Biju (E-mail: rajendran.biju@gmail.com) and C. P. Reghunadhan Nair (E-mail: cprnair@gmail.com)

ABSTRACT: The effect of phenol end functional shape memory oligomers on the shape memory properties of an epoxy-cyanate ester resin system was examined. The basic resin system consisted of diglycidyl ether of bisphenol A (DGEBA) cured with bisphenol A dicyanate (BADC). For conferring the shape memory properties, the switching segment (SS) components selected are α, ω-phenol-terminated poly(tetramethyleneoxide) (PPTMO), poly(ε-caprolactone) (PPCL), and poly(propylene glycol) (PPPG). Epoxy-cyanate ester blend of defined composition was analyzed for thermal, mechanical, thermo-mechanical, and shape memory properties at two concentrations of the three SSs. The transition temperature of heavily SS loaded matrix increased in the order: PPTMO < PPCL < PPPG commensurate with crystallizability of SS segments at ambient. For same reason flexural property showed an increasing trend. This is in league with the increased crystallizability of the shape memory polymer components. The shape fixity, recovery extent, and recovery time followed a reverse order: PPPG < PPCL < PPTMO. In contrast to the alcohol terminated shape memory components, phenol terminal groups were helpful in integrating the shape memory segments into the matrix by way of reaction with both epoxy and cyanate groups. The coreaction was conducive for achieving better shape memory properties and decreasing the transition temperature. A direct relation existed between the modulus ratio and the shape recovery property. Higher concentration of the SSs caused a diminution in transition temperature but enhanced the shape memory properties, though the mechanical properties were adversely affected. The shape recovery increased with increase in temperature. All polymers possessed good mechanical properties and thermal stability. © 2014 Wiley Periodicals, Inc. J. Appl. Polym. Sci. **2014**, *131*, 41196.

KEYWORDS: applications; crosslinking; stimuli-sensitive polymers

Received 12 April 2014; accepted 22 June 2014

DOI: 10.1002/app.41196

INTRODUCTION

The shape memory property (SMP) refers to the phenomenon of a material recovering its original shape at the presence of a stimulus after being severely and quasi-plastically distorted.[1–3] The SMP in polymeric materials can essentially be triggered by four basic types of stimuli, namely temperature variation (thermo-responsive); chemicals (chemo-responsive, including water, ethanol, and pH change etc.); light (photo-responsive, without apparent temperature fluctuation); and mechanical force (mechano-responsive, including impact, and pressure).[2–16]

Among these, the thermo-responsive systems are very common. There are three basic working mechanisms for the thermo-responsive SMP (i) dual-state mechanism (DSM), (ii) dual-composite mechanism (DCM), and (iii) partial-transition mechanism (PTM). In DSM, the distorted shape of polymer is maintained while cooling to below its glass transition range. Since the micro-Brownian motion is frozen in the glass state, the distorted shape can be largely maintained even after the constraint is removed. Heating back to room temperature, the system regains its rubbery state and thus the micro-Brownian motion is reactivated, which drives the polymer to recover its original shape. Alternately, the SMP can be imparted by having a hard/soft segment structure. If the hard segment or matrix is elastic within the temperature range of interest and then the soft segment or inclusion is able to significantly alter its stiffness when being heated by means of either the glass transition or melting. It is possible to realize the thermo-responsive shape memory properties in these DCM type polymers. The elastic matrix/segment forms the elastic component, while the soft segment is the transition component (switching segment, SS). After programming either at high or low temperatures, the elastic component stores elastic energy while the plastically distorted and (re-)hardened transition component provides constraint to prevent shape recovery at low temperatures. Reheating to soften the transition component removes the constraint and the stored elastic energy in the elastic component drives the polymer to return to its original shape. In the PTM series, instead of having

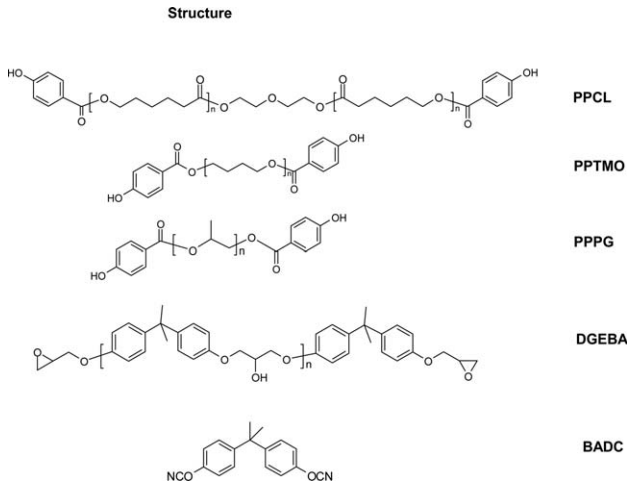

Scheme 1. Structure of different switching segments, epoxy, and cyanate ester.

a complete transition, heating may stop at a temperature within the transition range. As such, when deformed, the unsoftened portion serves as the elastic component to store elastic energy, while the softened portion behaves as the transition component. It is possible to alter the properties of a thermo-responsive shape memory polymer, such as the recovery temperature, shape fixity, shape recovery by means of selecting the programming temperature to achieve optimized performance.

Among the three, the DCM approach has been found to be very effective in conferring good shape memory properties to thermoset polymers, most of which inherently possesses this property by virtue of DSM mechanism. The soft segments can be either blended with or chemically attached to the base polymer. Adopting this strategy, several shape memory polymer systems containing shape memory segments (SS), such as poly(propylene glycol) (PPG), poly(ε-caprolactone) (PCL), poly(ethylene glycol) (PEG) etc. have been reported.[17–26] In earlier work, we extended this blending technique for deriving shape memory epoxy, epoxy-cyanate, bismaleimide resins etc.[27–29] These studies addressed mainly the dependency of the concentration of a given component (SS) on the shape memory properties of a matrix. However, a study of the comparative effect of various shape memory components in the shape memory properties of a given matrix has not been reported much. A few studies in these lines include; synthesis and shape memory properties of multiblock copolymers containing aramid hard segments and extended polycaprolactone soft segments.[30] Poly(caprolactone)-polyamide multiblock copolymers[31] and styrene-butadiene-styrene tri-block copolymer blends with PCL[32] have been reported as shape memory polymers. Shape memory polymer networks were prepared from blends of carboxylate telechelic PCL and epoxidized natural rubber.[33] In this series, a norbornene based copolymer with long PCL) side chain was synthesized.[34] Shape-memory polymer networks were derived using oligo-(caprolactone) dimethacrylate as crosslinker for *n*-butylacrylate.[35] Amorphous copoly(ether)ester networks based on oligo(propylene glycol) and oligo[(*rac*-dilactide)-*co*-glycolide] segments resulted in shape memory systems.[36] Many of these systems are reported to possess shape memory properties by virtue of the PCL or poly(propylene) segments incorporated chemically into the matrix. In a recent article, Kumar et al. examined the comparative shape memory properties of hydroxyl telechelic PEG, PPG, and poly(tetramethylene oxide) and found the superiority of PPG over the other two.[37] The shape memory components were partially reacted with the core matrix.

This article examines the effect of three shape memory components (SS) possessing phenol terminals on the mechanical, dynamic mechanical, and shape memory properties of an epoxy-cyanate ester resin system based on diglycidyl ether of bisphenol A (DGEBA) cured with bisphenol A dicyanate (BADC). Epoxy-cyanate ester blends are known for their strength, tunable mechanical properties and hydrophobicity and are suited for space deployable structures. The three components are: phenol-telechelic poly(tetramethylene oxide) (PPTMO), phenol telechelic poly(caprolactone) (PPCL), and phenol-telechelic poly(propylene glycol) (PPPG). Epoxy-cyanate ester blends with two compositions of SS i.e., DGEBA/SS/BADC (molar ratio-1/0.07/0.82 and 1/0.16/0.82) were chosen as the resin.

EXPERIMENTAL

Materials

Poly(tetramethylene oxide)diol (PTMOH), PCLdiol and PPG all with an average molecular weight $M_n = 2000$ g/mol were supplied by Aldrich Chemicals, USA. BADC was supplied by Lonza, Switzerland. Epoxy resin, DGEBA with an epoxy value 5.4 eq/kg (molecular weight 370 g/mol) was procured from Ciba Geigy, India. Zinc octate was supplied by Amirtha Industries, Mumbai, India. Nonyl phenol was purchased from Fluka, Switzerland, *para*-hydroxybenzoic acid (PHBA) from SRL chemicals, Mumbai, India and *para*-toluenesulfonic acid (pTSA) from CDH chemicals, Mumbai, India. Chloroform and toluene (supplied by SRL chemicals, Mumbai, India) were purified by distillation. Diglyme was purchased from Loba Chemie chemicals, Mumbai, India. Polyols and epoxy resin were dried in a flash evaporator at 80°C for 5 h before use. PHBA was dried in vacuum oven at 80°C for 3 h. Catalyst was prepared by mixing of zinc octate and nonyl phenol in a weight ratio of 3 : 40.

Synthesis of Phenol-Functional Oligomers

PPTMO was synthesized by reaction of poly(tetramethylene oxide)diol (PTMOH, 0.1 mol) with *para*-hydroxy benzoic acid (PHBA, 0.6 mol) in toluene/diglyme solvent in the presence of *para*-toluenesulfonic acid (pTSA, 2 wt %) as catalyst as reported earlier.[27] The mixture was refluxed for 20 h and the byproduct water was removed by azeotropic distillation using toluene in a Dean Stark apparatus. After completion of reaction, the solvent was removed by distillation and the resultant viscous material was dissolved in $CHCl_3$ and the unreacted PHBA was filtered out. The filtrate was washed several times with 5% $NaHCO_3$ solution to remove the catalyst and unreacted PHBA. The $CHCl_3$ solution was dried over anhydrous Na_2SO_4 for one day, filtered and the solvent was removed in a flash evaporator at 60°C. The resultant resin was characterized by fourier transform infrared spectroscopy (FTIR) and size exclusion chromatography (SEC). Estimation of ester value was done by chemical analysis. Same synthesis route was followed for PPCL and PPPG. Structure of various SSs, epoxy and cyanate ester are shown in Scheme 1. The PPTMO, PPCL, and PPPG are denoted as SS.

Synthesis of Shape Memory Epoxy-Cyanate Ester Resin

The DGEBA/SS/BADC blend and catalyst (zinc octate and nonyl phenol, 4 wt % of BADC) were first mixed together, degassed at 80°C for 30 min and then poured into a steel mold. Catalyst was separately prepared by mixing of zinc octate and nonyl phenol in a weight ratio of 3 : 40. The mold was heated in an air oven following the cure schedule as: 100°C for half hour, 120°C for 1 h, 150°C for 1 h, 180°C for 1 h and the final cure temperature was given as 200°C for 3 h. The mold was cooled slowly to ambient temperature. The cured polymer block was removed and cut to required dimensions for different testing. Blends of DGEBA and BADC with different SSs (PPTMO, PPCL, and PPPG) were prepared following the same procedure. Two compositions of DGEBA/SS/BADC with weight ratios, 50/20.5/30.5 and 38.5/37.8/23.6 (molar ratio-1/0.07/0.82 and 1/0.16/0.82) were selected in this study. Since all the three components of the base resins systems are difunctional, their molar ratios equal their equivalent ratios. For comparison, the epoxy resin and cyanate ester were cured in the same molar ratio (1 : 0.82) without any SS at 250°C for 3 h and evaluated for its shape memory properties.

Polymer Characterization

Fourier Transform Infrared Spectroscopy (FTIR). FTIR spectra were recorded on a Perkin-Elmer spectrum GXA model in the range of 4000–550 cm^{-1} with a resolution of 4 cm^{-1}.

Size Exclusion Chromatography (SEC), Gel Permeation Chromatography (GPC). The size exclusion chromatography was carried out with Waters alliance 2690 separation module in conjunction with Waters 410 differential refractive index detectors and UV detectors. The columns were Waters HR1 and HR2 Styragel columns. SEC columns were calibrated with polystyrene standards.

Differential Scanning Calorimetry (DSC) and Thermo Gravimetric Analysis (TGA). DSC and TGA were carried out using a Mettler DSC Q20. For DSC analysis, the samples were heated from room temperature to 300°C at a heating rate 5°C/min in N_2 atmosphere and TGA was done from room temperature to 600°C at a heating rate 10°C/min in N_2 atmosphere.

Flexural Strength. Flexural strength was determined at room temperature by three-point bending testing as per the standard ASTM D790 using a UTM (Instron Model 5569). Specimen size used is 3.2 × 12.7 × 125 mm^3. Strain rate is 0.01 (mm/mm)/min.

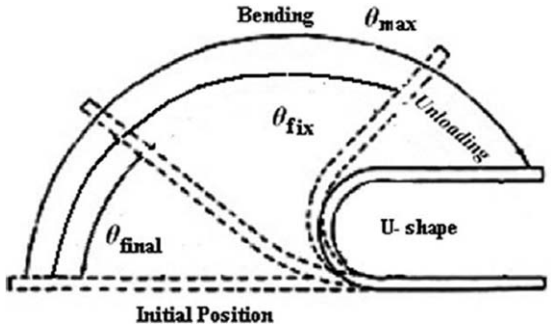

Scheme 2. Schematic representation of bending test. [Color figure can be viewed in the online issue, which is available at wileyonlinelibrary.com.]

Dynamic Mechanical Thermal Analysis (DMA). Dynamic mechanical properties and transition temperatures (T_{trans}) were determined using TA instruments DMA Q800 in the three point bending mode at a frequency 1 Hz and a heating rate 3°C/min. The T_{trans} was taken as the temperature corresponding to the maximum in Tanδ-temperature graph.

Bending Test

A straight rectangular strip of polymer of size 120 × 15 × 2.6 (mm) was used for the test. The test was done by initially heating the sample above its T_{trans} followed by deforming (sample was bent into "U shape" and stress was applied using hands, then held for 10 s) and then fixing the shape by cooling below its T_{trans} (sample cooled in an ice bath for 20 s after sealing it in a thin polypropylene cover). The heating was done in a temperature controlled air oven provided with a glass window. The tweezers were used as shaft for holding the sample and to bend the sample, stress was applied by the hands on tweezers. The maximum angle of bending was measured as θ_{max} (in this case maximum strain is 30°). The resultant deformation was measured as angle (θ_{fixed}). Then the shape fixed sample was immediately kept in a glass window air oven set at the required temperature and the time needed to recover the shape was noted (about 1 min is required for the sample to attain the oven temperature, which is deduced from the total recovery time). After that the sample was taken out and the bending angle (θ_{final}) was noted.[28,38] The schematic representation of

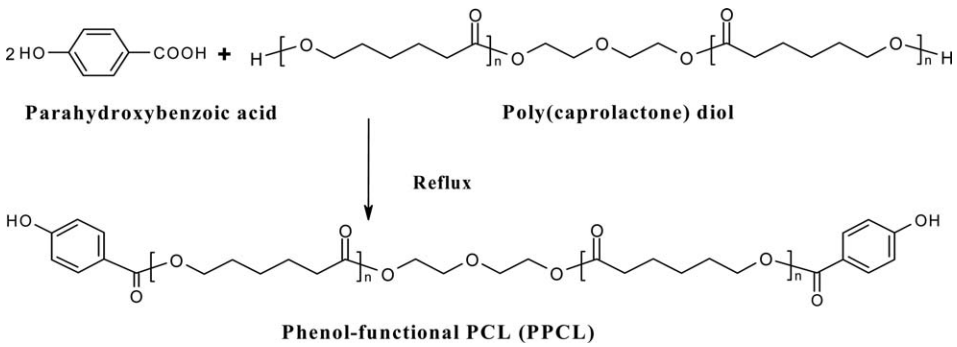

Scheme 3. Synthesis of PPCL. [Color figure can be viewed in the online issue, which is available at wileyonlinelibrary.com.]

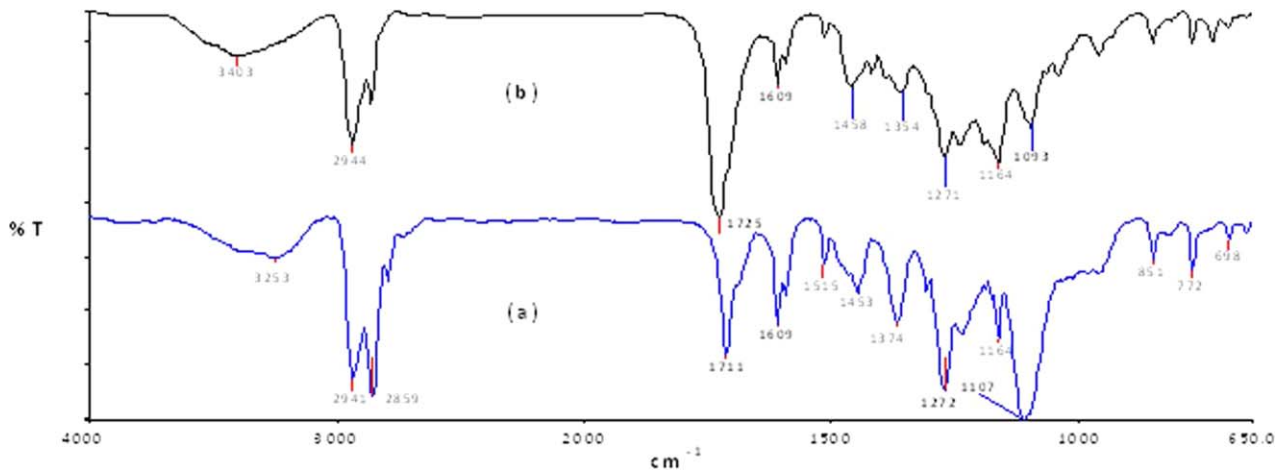

Figure 1. FTIR spectrum of (a) PPPG and (b) PPCL. [Color figure can be viewed in the online issue, which is available at wileyonlinelibrary.com.]

bending test was shown in Scheme 2. The oven temperature was maintained at T_{trans} +20°C. The time needed to attain the angle θ_{final} was taken as recovery time. The above test was repeated thrice and average recovery time was taken.

$$\text{Shape recovery } (\%) = [(\theta_{max} - \theta_{final})/\theta_{max}] \times 100 \quad (1)$$

$$\text{Shape retention } (\%) = [\theta_{fixed}/\theta_{max}] \times 100 \quad (2)$$

Since the sample is subjected to flexural strain during the bend test, the flexural strain can be approximated as: half Lx tanθ, where, L is the length of the sample. The maximum programmed strain in this case is ~35% ($^1/_2$tan30).

RESULTS AND DISCUSSION

The base polymer system consisted of a blend of cyanate ester and epoxy resin along with the phenol functional oligomer of poly(tetramethylene oxide), PPG or PCL as the shape memory component. The molar ratio of cyanate ester and epoxy resin was maintained as 0.82 : 1.0. Two compositions containing 20 and 38 wt % of each SS were investigated for their shape memory properties.

In the following discussion, PTMOH, PTMO, and PPTMO refer to poly(tetramethylene oxide) diol, poly(tetramethylene oxide) segment and phenol terminated polytetramethylene oxide, respectively.

Synthesis of α, ω-Phenol Functional Switching Segments

The phenol functional shape memory SS were synthesized from their hydroxyl telechelics by reaction with *para*-hydroxy benzoic acid (PHBA) using pTSA as catalyst. Same method of synthesis and characterization were adapted for PPPG and PPTMO. The typical synthesis of PPCL is illustrated in Scheme 3 and typical FTIR spectra of PPCL and PPPG are shown in Figure 1. The peak at 3419 cm^{-1} corresponds to stretching vibration of —OH groups and that at 1725 cm^{-1} to the C═O stretching of the ester group. The peak at 1164 cm^{-1} corresponds to C—O—C stretching. The polymer was further characterized by ester value estimation. The ester value of PPCL (47 mgKOH/g) conformed nearly to the theoretical value (49.3 mgKOH/g). The OH terminated oligomers are

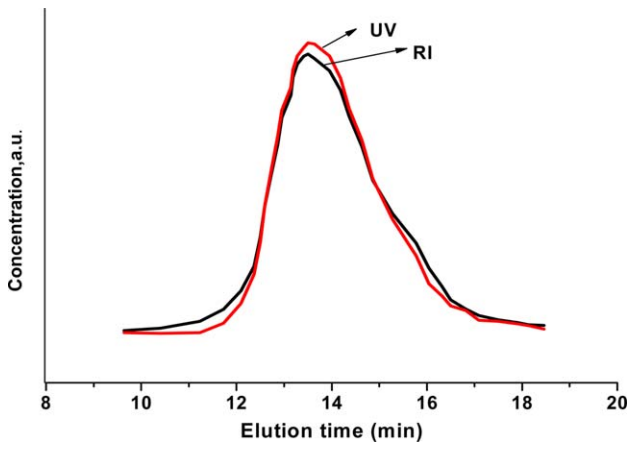

Figure 2. SEC profiles of PPCL (Superimposition of RI and UV detected traces). [Color figure can be viewed in the online issue, which is available at wileyonlinelibrary.com.]

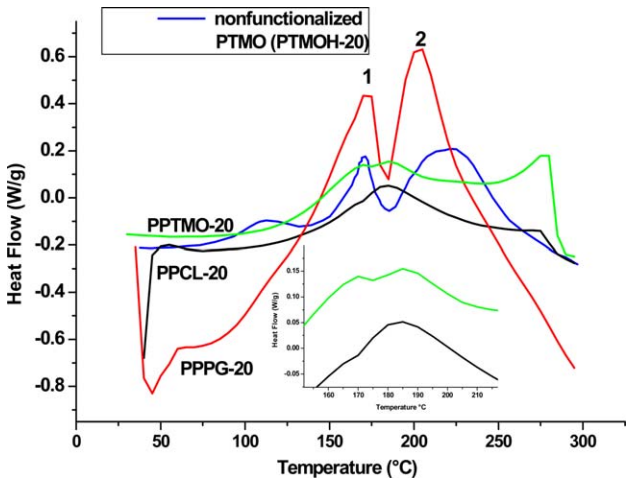

Figure 3. DSC profile of different systems. [Color figure can be viewed in the online issue, which is available at wileyonlinelibrary.com.]

Table I. Composition of the Ternary Blend, DSC Exotherm Peak Maxima of Epoxy-Cyanate Ester Systems Containing Different Switching Segments

			DSC data	
Sample	Molar ratio of DGEBA/SS/BADC	Mass ratio of DGEBA/SS/BADC	Peak max 1 (°C)	Peak max 2 (°C)
PTMOH-20[a]	1/0.07/0.82	50.2/19.0/30.8	170	225
PPTMO-20	1/0.07/0.82	50/20.5/30.5	170	185
PPCL-20	1/0.07/0.82	50/20.5/30.5	-	183
PPPG-20	1/0.07/0.82	50/20.5/30.5	169	203
PPTMO-38	1/0.16/0.82	38.5/37.8/23.6	177	-
PPCL-38	1/0.16/0.82	38.5/37.8/23.6	158	210
PPPG-38	1/0.16/0.82	38.5/37.8/23.6	175	216

[a] Nonfunctionalized.

not UV sensitive. However, the end capping phenolic moieties are UV sensitive. This makes the polymer sensitive to UV and can be detected in SEC (GPC) by UV detector in addition to refractive index detector. If the chains are not functionalized with phenol groups uniformly, the SEC profile by both and UV detection will look different. The SEC profiles of the phenol functional oligomers by both refractive index and UV detector techniques showed almost similar pattern. This implies that all polymer chains (irrespective of molecular weight) are uniformly end-capped with phenolic groups (see Figure 2, typically for PPCL).

Cure Characterization

The cure characterization of DGEBA/PPTMO/BADC blend has been reported earlier.[27] The cure schedule of the DGEBA/PPPG/BADC and DGEBA/PPCL/BADC blends was determined by DSC and FTIR. The DSC profiles (Figure 3) of the PPPG system show one exotherm at 170°C and another at 203°C (data in Table I). The exotherm at 170°C is attributed to cyanate-epoxy reaction leading to the formation of oxazolidinone groups[39] and that at 203°C to the polymerization of cyanate groups.[40] Both PPTMO and PPCL systems showed broad exotherms from 140 to 240°C with one T_{max} at 183°C and another at 205°C encompassing both these reactions.

The DSC profile of the blend containing nonfunctionalized PTMOH (PTMOH-20, DGEBA/PTMOH/BADC) shows same trend as the phenol functionalized systems. The exotherm (Figure 3) at 170°C is attributed to the formation of oxazolidinone groups and that at 225°C to the polymerization of cyanate groups. While the cyanate ester polymerization in the nonfunctionalized PTMOH blend occurred at high temperature (225°C), the blends containing phenol functional polymers showed this exotherm at a lower temperature due to the involvement of the phenolic groups in the catalysis of cyanate ester homopolymerzation. It is possible that the phenol groups react with epoxy resin also. Alcohol groups are also known to catalyst cyanate polymerization though less effective than phenols.[37]

Similar results were obtained in higher shape memory component containing systems such as PPCL-38 and PPPG-38 (SS content 38%) as those obtained in the case of PPCL-20 and PPPG-20 (SS content 20%) as discussed above. The possible reaction mechanism of coreaction of epoxy resin with cyanate ester and PPTMO as reported earlier.[27]

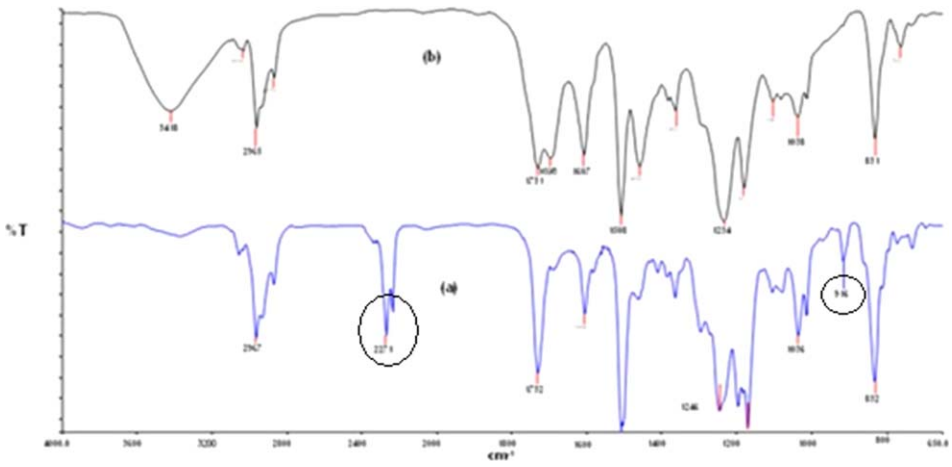

Figure 4. FTIR Spectra of PPCL-20 (a) uncured and (b) cured blend (200°C, 3 h). [Color figure can be viewed in the online issue, which is available at wileyonlinelibrary.com.]

Table II. Flexural Strength, T_{trans}, Elastic Modulus Ratio and Shape Memory Properties of Different Systems

Sample	Flexural Strength (MPa)	T_{trans} (°C)	E_g/E_r	% of shape recovery at T_{trans} + 20 (°C)	Recovery time (min)	% of shape fixity at T_{trans}−20 (°C)
PTMOH-20[a]	89 ± 0.5	139	12	85	3.00	85
PPTMO- 20	100 ± 0.5	107	17	90	2.50	98
PPCL-20	98 ± 0.5	120	15	87	2.55	92
PPPG-20	95 ± 0.5	157	10.4	80	3.10	80
PPTMO-38	14 ± 0.5	72	23	98	1.30	97
PPCL-38	23 ± 0.5	55	20	98	1.20	94
PPPG-38	32 ± 0.5	128	14	93	2.10	90

[a] Nonfunctionalized.

From FTIR, (Figure 4) completion of cure reaction of the epoxy and —OCN groups in the network was confirmed from the absence of peaks corresponding to epoxy ring at 916 cm^{-1} and of —OCN at 2271–2238 cm^{-1}. It was further confirmed from the appearance of triazine peaks at 1363 cm^{-1} and of isocyanurate at 1698 and 1459 cm^{-1}.[41] The oxazolidinone ring formed from the reaction of cyanate and epoxy was observed at 1731 cm^{-1}.[42,43] Following the above studies, all the compositions were cured under the cure schedules: 100°C for half hour, 120°C for 1 h, 150°C for 1 h, 180°C for 1 h, and 200°C for 3 h.

Flexural Properties

Table II compiles the flexural strength of the different resin blends. The flexural strength shows more or less same value for all the three systems at SS concentration of 20%. An increasing trend was observed at high SS content in the order, PPTMO-38 < PPCL-38 < PPPG-38. The flexural strength is practically invariant for all the three systems at 20% loading of the SS component. At this concentration, all the three additives are well dispersed in the base matrix and they effectively plasticize the matrix. However, at 38% SS loading there is a possibility for the SS to phase separate and crystallize in the matrix. The crystalline melting points of the three SS (for molecular weight of 2000) are: PPCL +50°C, PPPG −31°C, and PPTMO +20°C. At the test conditions of 25°C, only PPCL and PPTMO will have the SS segments in crystallized state. Therefore, these systems show lower flexural strength at 38% loading when compared to PPPG (Table II).

The flexural strength of nonfunctionalized PTMOH (PTMOH-20) is lower than that of phenol functionalized PTMO (PPTMO-20). The reactive SS provide the epoxy-cyanate ester more flexibility by increasing the spacing between crosslinks and this helps improve its SMP too (discussed later).

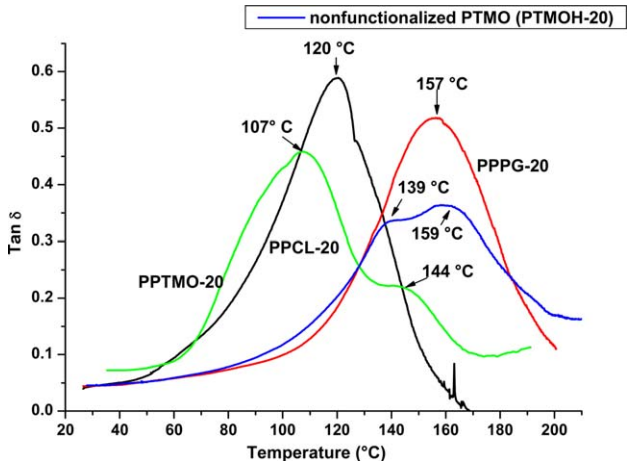

Figure 5. Loss tangent (tanδ)-temperature profile for low switching content (20%) systems. (The T_{trans} was taken as the temperature corresponding to the maximum in the tanδ-temperature graph. The prominent peak was considered). [Color figure can be viewed in the online issue, which is available at wileyonlinelibrary.com.]

Dynamic Mechanical Thermal Properties

Visco-elastic properties of the samples were investigated by DMA in three point bending mode. Figures 5 and 6 indicate the loss tangent (tanδ) for different systems as a function of temperature. The transition temperature (T_{trans}) was determined from the tanδ peak. The modulus ratio E_g/E_r is taken as ($E'_{Ttrans-20}/E'_{Ttrans+20}$). Where, $E'_{Ttrans-20}$ and $E'_{Ttrans+20}$ stand for the storage modulus at temperatures $T_{trans-20}$ and $T_{trans+20}$, respectively. At lower temperature, PPCL-20 shows higher storage modulus than other two systems, but it suddenly drops after 80°C. Beyond this temperature, PPPG-20 shows higher modulus than both PPCL-20 and PPTMO-20. While the storage

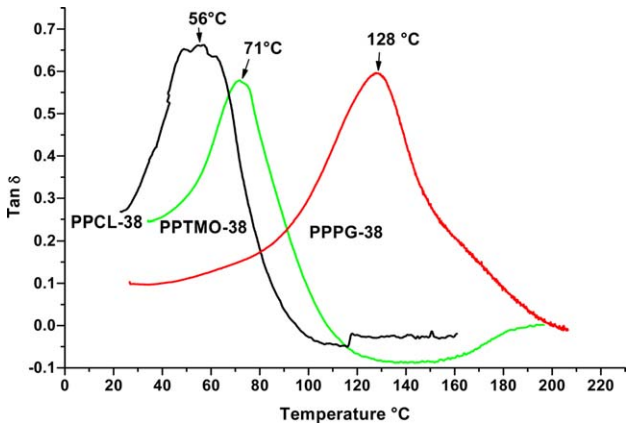

Figure 6. Loss tangent (tanδ)-temperature profile for high switching content (38%) systems. [Color figure can be viewed in the online issue, which is available at wileyonlinelibrary.com.]

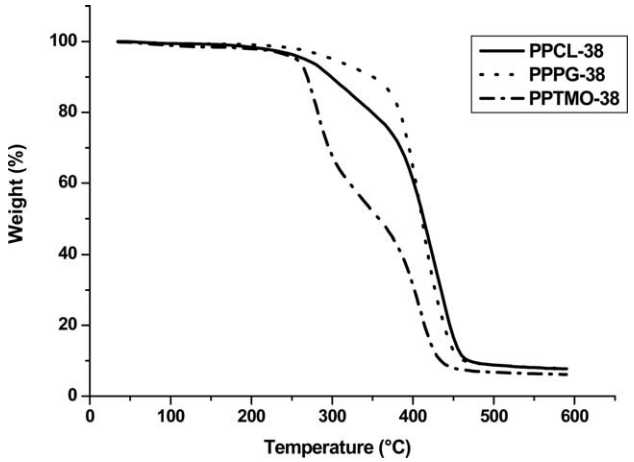

Figure 7. TGA traces of systems with 38% switching segments loading (N_2, 10°C/min).

modulus decreases, the E_g/E_r ratio (Table II) increases in the order PPPG-20 < PPCL-20 < PPTMO-20. The transition temperatures are in the order viz: PPTMO-20 < PPCL-20 < PPPG-20 showing a reverse trend of storage modulus. The high transition temperature (Fig. 6) of PPPG-20 is due to crystalline nature of this segment when compared to other two systems. PPCL contains longer aliphatic chain and an ester group and provides more dipolar interaction of the chain segments. But in PPTMO, this type of interaction is comparatively less probable as it is gifted only with ether groups spaced between four —CH_2— groups. PCL has, therefore, better crystallizability than PTMO explaining the superiority of the former in forming a stronger matrix with comparatively higher T_{trans}.

Similar trend in storage modulus is observed in high SS content viz: PPTMO-38, PPCL-38, and PPPG-38. The transition temperature shows the trend PPTMO-38 < PPCL-38 < PPPG-38. This is again in league with the crystallizability of the shape memory polymer component. The transition temperature of PTMOH-20 (139°C) is higher than that of PPTMO-20 (100°C)

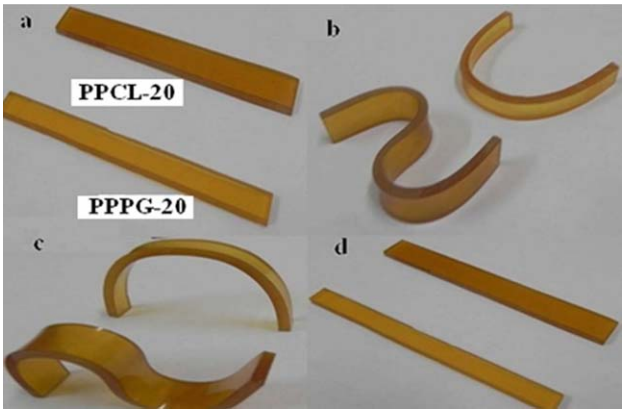

Figure 8. Shape memory properties of PPCL-20 and PPPG-20 (a) original/permanent shapes, (b) and (c) fixed temporary shapes and (d) recovered shapes. [Color figure can be viewed in the online issue, which is available at wileyonlinelibrary.com.]

system. This is clear that nonfunctionalized PTMOH (alcohol terminal) is less reactive than functionalized PTMO (phenol terminal). In this case, PTMO segments are unlikely to alter the crosslink density of the epoxy-cyanate ester matrix by way of coreaction. In other words, matrix plasticization by free PTMOH is less probable than by the co-reacted PPTMO at lower concentration. In case of both OH and phenol functional PTMO, the matrix shows a dual phase behavior. The one at low temperature is due to the oxazolidinone rich phase and that at high temperature due to triazine rich phase. Both containing PTMO either physically blended (for PTMOH-20) or chemically integrated (for PPTMO-20). In the reacted case, the two transitions occur at relatively lower temperature. As the PTMO content increases to 38%, it converges to a single oxazolidinone phase appearing at lower temperature 70°C.

Thermo Gravimetric Analysis (TGA)

Figure 7 represents the typical TGA of the cured compositions containing 38% shape memory component. All the three systems showed thermal stability above 280°C. The cyanate ester-epoxy system alone normally decomposes at temperature >350°C.[44] Additions of the shape memory components diminish the thermal stability. Among the three, PPPG caused least damage for the thermal stability, while PPTMO made the system thermally least stable. Practically, all the PPTMO degraded at around 300°C. However, all the systems have stability well above their service temperature (normally around the transition temperature).

Shape Memory Properties (Bending Test)

Qualitatively, the shape memory behavior was estimated by bending test between the temperatures (T_{trans} + 20°C) and (T_{trans} − 20°C). The shape memory studies are done with respect to the transition temperature. By virtue of the DSM mechanism, the epoxy-cyanate system as such shows some shape memory properties. The epoxy-cyanate ester matrix without any SS was cured at 250°C and it showed a T_{trans} of 223°C.[37] However, its shape retention was only 82% and shape recovery was poor (64%).

The shape memory behaviors of PPCL-20 and PPPG-20 are demonstrated in Figure 8. Those of PPTMO-20 have been discussed earlier.[27] The original (permanent) rectangular shape (a) was heated at T_{trans} + 20°C and the sample was deformed into different shapes through bending and twisting. Upon cooling under load, these deformed temporary shapes (b) and (c) were fixed. On reheating above T_{trans}, the sample recovered its original rectangular shape (d). The recovered shape was practically indistinguishable from the original shape, confirming the excellent shape fixity and recovery.

For quantitative evaluation, the bending tests of all systems were conducted at temperatures T_{trans} + 20°C (Table II). At T_{trans} + 20°C the shape recovery of low SS content system increases in the order PPPG-20 < PPCL-20 < PPTMO-20. This observation conforms to the trend in modulus ratio (E_g/E_r), which increases in the same manner as has been observed in previous studies also.[45] At high E_g/E_r ratio, the shape recovery is maximum at minimal recovery time. There is a linear relationship between E_g/E_r ratio and extent of shape recovery though it deals with three different systems, as shown in Figure 9. The

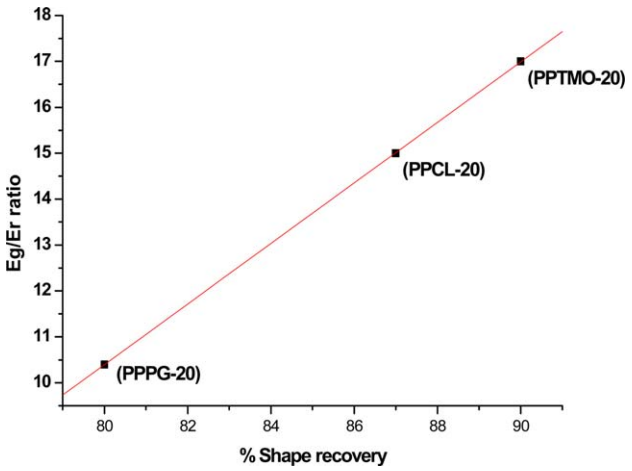

Figure 9. Variation of E_g/E_r with % shape recovery for different at 20% of switching segments. [Color figure can be viewed in the online issue, which is available at wileyonlinelibrary.com.]

highly crosslinked structures have strong restraining force on their segments, which need large free volume and more energy, necessarily higher temperature to accomplish shape recovery.[46]

In all cases, the shape fixity and recovery time are marginally better for PPTMO, while the PPPG system is inferior to the other two in terms of shape fixity, shape recovery, and time needed for recovery. It is concluded that both PPCL and PPTMO are good shape memory conferring segments while PPPG is not rated good for the same. The effect of phenol end group was examined by comparing the properties of a typical system containing the same effective concentration of alcohol telechelic polytetramethylene oxide. This system also manifested shape memory characteristics as reported earlier.[37]

However, it showed comparatively poor shape retention and recovery and a lower E_g/E_r ratio. The recovery time was marginally more despite a high T_{trans} of 130°C for this system (Table II). This difference can be ascribed to the lack of incorporation of sufficient shape memory component in the epoxy-cyanate ester matrix by way of coreaction. It is inferred that coreaction of the shape memory component in the matrix is conducive for achieving good shape memory properties. Higher concentration of the SS causes a diminution in transition temperature but improves the shape memory characteristics in terms of enhanced shape recovery and fixity and diminished recovery time, though the mechanical properties are adversely affected. All systems are mechanically sturdy and have good thermal stability to be used in composites for developing smart system for diverse application.

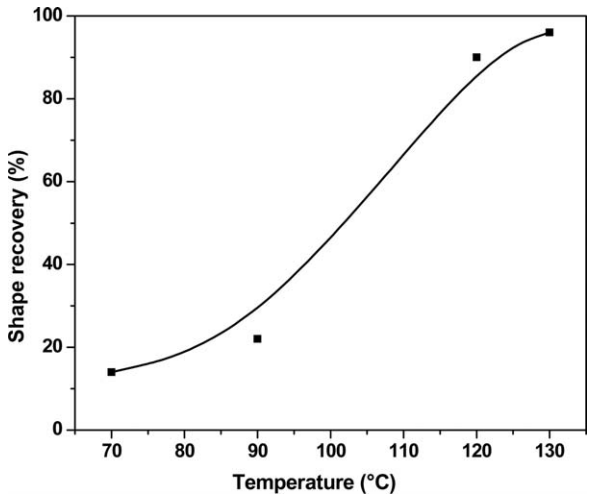

Figure 10. Dependency of shape recovery with temperature (recovery duration 3 min).

Stress Relaxation and Temperature Dependency of Shape Memory Properties

Since polymers are viscoelastic in nature, the stored energy during shape fixing can be relaxed by way of stress relaxation depending on the temperature at which the fixed component is kept. A detailed study of stress relaxation of a typical system PPTMO-20 was already reported by us.[47] These studies were carried out by cyclic DMA method. The stress relaxation was fast above the transition temperature. The system showed some relaxation even below the T_{trans}. Relaxation modulus decayed exponentially with time and the modules was maximum at 70°C and minimum at 130°C ($T_{switch} + -30$°C). The computed relaxation time decreased drastically with rise in temperature. The dependency of shape recovery on temperature is shown in Figure 10. As stress relaxation has a direct relation to the shape fixity and the shape recovery characteristics, the shape recovery was studied in the temperature range 70–130°C. Shape recovery of 14% was observed at 70°C. It increased to 22% at 90°C and to 90% at 120°C. At 130°C, the recovery was 96%. In all cases the system was allowed to relax for 3 min. The increase in shape recovery is promoted by thermally activated segmental motion. This implies the need for storing the shape memory polymers well below the T_{trans} to preclude inadvertent loss in shape due to stress relaxation.

CONCLUSIONS

The role of three SS on the SMP of epoxy-cyanate ester system was investigated. The shape memory thermoset polymer was derived by coreacting cyanate ester and epoxy resin with phenol-telechelics of different SS constituted by PPTMO, PPCL, and PPPG. Phenol groups help the shape memory component get integrated into the network matrix through coreaction with both cyanate and epoxy groups. The transition temperature shows the trend PPTMO < PPCL < PPPG. This is in league with the crystallizability of the shape memory polymer additives, which increases in the same order. In all cases, the shape fixity and recovery extent and recovery time are better for PPTMO than for PPCL. PPPG system is inferior to the other two in terms of these properties. The extent of shape recovery increased with recovery temperature. All polymer possessed good mechanical properties and thermal stability. In contrast to the alcohol terminated shape memory component, phenol terminal groups help the SS get integrated into the matrix by way of reaction that decreases the transition temperature. This helps in achieving better shape memory properties. Higher concentration of the SS causes a diminution in transition temperature but improves the shape memory characteristics, though the

mechanical properties are adversely affected. The resins are suited to process good elastic memory composites as cyanate esters normally promote excellent composite formation.

ACKNOWLEDGMENTS

The authors are grateful to Director VSSC for permission to publish the article. Analytical support from colleagues in Analytical and Spectroscopy Division is gratefully acknowledged. The authors are grateful to Dr. K. M. Usha for critically reviewing this article.

REFERENCES

1. Otsuka, K.; Wayman, C. M. Shape Memory Materials; Cambridge University Press: Cambridge, UK, **1998**; pp 36–38.
2. Huang, W. M.; Ding, Z.; Wang, C. C.; Wei, J.; Zhao, Y.; Purnawali, H. *Mater. Today* **2010**, *13*, 54.
3. Huang, W. M.; Zhao, Y.; Wang, C. C.; Ding, Z.; Purnawali, H.; Tang, C.; Zhang, J. L. *J. Polym. Res.* **2012**, *19*, 9952.
4. Lendlein, A. Shape-Memory Polymers; Springer-Verlag: Heidelberg, Germany, **2010**.
5. Sun, L.; Huang, W. M.; Ding, Z.; Zhao, Y.; Wang, C. C.; Purnawali, H.; Tang, C. *Mater. Des.* **2012**, *33*, 577.
6. Zhao, Q.; Kelch, S.; Lendlein, A. *Soft Matter.* **2013**, *9*, 1744.
7. Mather, P. T.; Luo, X. F.; Rousseau, I. A. *Annu. Rev. Mater. Res.* **2009**, *39*, 445.
8. Xie, T. *Polymer* **2011**, *52*, 4985.
9. Wang, C. C.; Huang, W. M.; Ding, Z.; Zhao, Y.; Purnawali, H. *Compos. Sci. Technol.* **2012**, *72*, 1178.
10. Yakacki, C. M.; Satarkar, N. S.; Gall, K.; Likos, R.; Hilt, J. Z. *J. Appl. Polym. Sci.* **2009**, *112*, 3166.
11. Lu, H. B. *J. Appl. Polym. Sci.* **2012**, *123*, 1137.
12. Zhu, Y.; Hu, J. L.; Luo, H. S.; Young, R. J.; Deng, L. B.; Zhang, S.; Fan, Y.; Ye, G. D. *Soft Matter.* **2012**, *8*, 2509.
13. Beloshenko, V. A.; Varyukhin, V. N.; Voznyak, Y. V. *Russ. Chem. Rev.* **2005**, *74*, 265.
14. Razzaq, M. Y.; Behl, M.; Lendlein, A. *Adv. Funct. Mater.* **2012**, *22*, 184.
15. Luo, X. F.; Mather, P. T. *Soft Matter* **2010**, *6*, 2146.
16. He, Z. W.; Satarkar, N.; Xie, T.; Cheng, Y. T.; Hilt, J. Z. *Adv. Mater.* **2011**, *23*, 3192.
17. Sheng, Z.; Yu, Z.; Govender, T.; Luo, H.; Li, B. *Polymer* **2008**, *49*, 3205.
18. Shim, Y.-S.; Chun, B.-C.; Chung, Y.-C. *Fibers Polym.* **2006**, *7*, 328.
19. Niu, Y.; Zhang, P.; Zhang, J.; Xiao, L.; Yang, K.; Wang, Y. *Polym. Chem.* **2012**, *3*, 2508.
20. Xue, L.; Dai, S.; Li, Z. *Biomaterials* **2010**, *31*, 8132.
21. Zhang, D.; Giese, M. L.; Prukop, S. L.; Grunlan, M. A. *J. Polym. Sci. Part A: Polym. Chem.* **2011**, *49*, 754.
22. Ajili, S. H.; Ebrahimi, N. G.; Soleimani, M. *Acta Biomater.* **2009**, *5*, 1519.
23. Yongkang, B.; Cheng, J.; Wang, Q.; Wang, T. *Carbohydr. Polym.* **2013**, *96*, 522.
24. Zia, K. M.; Zuber, M.; Barikani, M.; Bhatti, I. A.; Khan, M. B. *Colloids Surf. B* **2009**, *72*, 248.
25. Guo, B.; Chen, Y., Lei, Y.; Zhang, L.; Zhou, W. Y.; Rabie, A. B.; Zhao, J. *Biomacromolecules* **2011**, *12*, 1312.
26. Lendlein, A.; Schmidt, A. M.; Schroeter, M.; Langer, R. *J. Polym. Sci. Part A: Polym. Chem.* **2005**, *43*, 1369.
27. Biju, R.; Gouri, C.; Nair, C. P. R. *Eur. Polym. J.* **2012**, *48*, 499.
28. Biju, R.; Nair, C. P. R. *High Perform. Polym.* **2013**, *25*, 464.
29. Biju, R.; Nair, C. P. R. *J. Polym. Res.* **2013**, *20*, 1.
30. Schuh, C.; Schuh, K.; Lechmann, M. C.; Garnier, L.; Kraft, A. *Polymer* **2010**, *2*, 71.
31. Lee, H. Y.; Jeong, H. M.; Lee, J. S.; Kim, B. K. *Polym. J.* **2000**, *32*, 23.
32. Heng, Z.; Haitao, W.; Wei, Z.; Qiangguo, D. *Polymer* **2009**, *50*, 1596.
33. Chang, Y.-W.; Eom, J.-P.; Kim, J.-G.; Kim, H.-T.; Kim, D.-K. *J. Indus. Eng. Chem.* **2010**, *16*, 256.
34. Dan, Y.; Wei, H.; Jiahui, Y.; Jisen, J.; Liya, Z.; Xie, M. *Polymer* **2010**, *51*, 5100.
35. Lendlein, A.; Annette, M. S.; Robert, L. *Proc. Natl. Acad. Sci.* U S A **2001**, *98*, 842.
36. Zotzmann, J.; Alteheld, A.; Behl, M.; Lendlein, A. *J. Mater. Sci.: Mater. Med.* **2009**, *20*, 1815.
37. Kumar, K. S. S.; Khatwa, A. K.; Nair, C. P. R. *React. Funct. Polym.* **2014**, *78*, 7.
38. Lin, J. R.; Chen, L. W. *J. Appl. Polym. Sci.* **1998**, *69*, 1563.
39. Martin, M. D.; Ormaetxea, M.; Harismendy, I.; Remiro, P. M.; Mondragon, I. *Eur. Polym. J.* **1999**, *35*, 57.
40. Hamerton, I.; Hay, N. J. *High Perform. Polym.* **1998**, *10*, 163.
41. Zeng, M.; Lu, C.; Wang, B.; Qi, C. *Radiat. Phys. Chem.* **2010**, *79*, 966.
42. Lakshmi, M. S.; Reddy, B. S. R. *Eur. Polym. J.* **2002**, *38*, 795.
43. Nair, C. P. R.; Mathew, D.; Ninan, K. N. *Adv. Polym. Sci.* **2001**, *155*, 1.
44. Mathew, D.; Nair, C. P. R.; Ninan, K. N. *J. Appl. Polym. Sci.* **1999**, *74*, 1675.
45. Merline, D. J.; Nair, C. P. R.; Ninan, K. N. *J. Macromol. Sci.: Pure Appl. Chem.* **2008**, *45*, 312.
46. Liu, Y.; Han, C.; Tan, H.; Du, X. *Mater. Sci. Eng. A* **2010**, *527*, 2510.
47. Biju, R.; Kumar, K. S. S.; Rajeev, R. S.; Nair, C. P. R. *Polym. Adv. Technol.* **2013**, *24*, 623.